JCI The Journal of Clinical Investigation

Energetics of acute pressure overload of the porcine right ventricle. In vivo 31P nuclear magnetic resonance.

G G Schwartz, … , B Massie, M W Weiner

J Clin Invest. 1992;89(3):909-918. https://doi.org/10.1172/JCI115671.

Research Article

In vivo 31P nuclear magnetic resonance (NMR) spectroscopy of the right ventricular (RV) free wall was employed to determine (a) whether phosphorus energy metabolites vary reciprocally with workload in the RV and (b) the mechanisms that limit RV contractile function in acute pressure overload. In 20 open-chest pigs, phosphocreatine (PCr)/ATP ratio (an index of energy metabolism inversely related to free ADP concentration), myocardial blood flow (microspheres), and segment shortening (sonomicrometry, n = 14) were measured at control (RV systolic pressure 31 +/- 1 mm Hg), and with pulmonary artery constriction to produce moderate pressure overload (RV systolic pressure 45 +/- 1 mm Hg), and maximal pressure overload before overt RV failure and systemic hypotension (RV systolic pressure 60 +/- 1 mm Hg). With moderate pressure overload, PCr/ATP declined to 89% of control (P = 0.01), while contractile function increased. Adenosine (n = 10, mean dose 0.16 mg/kg-min) increased RV blood flow by an additional 41% without increasing PCr/ATP, indicating that coronary reserve was not depleted and that the decrease in PCr/ATP from control was not due to ischemia. With maximal pressure overload and incipient RV failure, PCr/ATP fell further to 81% of control and RV blood flow did not increase further, even with adenosine. Thus: (a) The decline in PCr/ATP with moderate RV pressure overload, without evident ischemia or contractile […]

Find the latest version:

https://jci.me/115671/pdf

Energetics of Acute Pressure Overload of the Porcine Right Ventricle

In Vivo ^{31}P Nuclear Magnetic Resonance

Gregory G. Schwartz, Sean Steinman, Jorge Garcia, Clifford Greyson, Barry Massie, and Michael W. Weiner
Cardiology Section and Magnetic Resonance Unit, San Francisco VA Medical Center, and Cardiovascular Research Institute and Department of Medicine, University of California, San Francisco, California 94121

Abstract

In vivo ^{31}P nuclear magnetic resonance (NMR) spectroscopy of the right ventricular (RV) free wall was employed to determine (*a*) whether phosphorus energy metabolites vary reciprocally with workload in the RV and (*b*) the mechanisms that limit RV contractile function in acute pressure overload. In 20 open-chest pigs, phosphocreatine (PCr)/ATP ratio (an index of energy metabolism inversely related to free ADP concentration), myocardial blood flow (microspheres), and segment shortening (sonomicrometry, $n = 14$) were measured at control (RV systolic pressure 31±1 mm Hg), and with pulmonary artery constriction to produce moderate pressure overload (RV systolic pressure 45±1 mm Hg), and maximal pressure overload before overt RV failure and systemic hypotension (RV systolic pressure 60±1 mm Hg). With moderate pressure overload, PCr/ATP declined to 89% of control ($P = 0.01$), while contractile function increased. Adenosine ($n = 10$, mean dose 0.16 mg/kg-min) increased RV blood flow by an additional 41% without increasing PCr/ATP, indicating that coronary reserve was not depleted and that the decrease in PCr/ATP from control was not due to ischemia. With maximal pressure overload and incipient RV failure, PCr/ATP fell further to 81% of control and RV blood flow did not increase further, even with adenosine. Thus: (*a*) The decline in PCr/ATP with moderate RV pressure overload, without evident ischemia or contractile dysfunction, supports the positive regulation of oxidative phosphorylation by ATP hydrolysis products. (*b*) Depletion of RV coronary flow reserve accompanies the onset of RV failure at maximal pressure overload. (*J. Clin. Invest.* 1992. 89:909–918.) Key words: coronary circulation • energy metabolism • myocardial contraction • pulmonary artery • pulmonary heart disease

Introduction

The relationships between energy metabolism, blood flow, and mechanical function of the left ventricle have been studied extensively in recent years (1, 2). Nuclear magnetic resonance (NMR)[1] spectroscopy has been an important tool in many of these investigations, providing a repetitive, nondestructive assessment of key myocardial metabolites.

In contrast, little is known of the energetics of the right ventricle (RV) in vivo. In addition to major differences in the structure, function, and perfusion of the two ventricles, there is considerable in vitro evidence of biochemical dissimilarities, suggesting differences in both the generation and utilization of chemical energy. For example, the RV has been found to have a lower mitochondrial density (3), a lower maximal rate of substrate oxidation (4), lower activities of lactate dehydrogenase (5) and creatine kinase (6), and a higher ratio of α/β myosin heavy chain isoforms (7, 8). These differences may represent adaptations to the lower metabolic requirements of the RV.

The goals of the current study were both methodologic and physiologic. The methodologic goal was to develop and implement techniques for in vivo ^{31}P NMR spectroscopy of the RV in an intact animal model. To date, NMR spectroscopy has not been employed to investigate RV energetics, in part because of difficulty obtaining sufficient NMR signal from the thin RV free wall. The NMR signal obtained in previous studies with a transvenous catheter coil (9) arose predominantly from the interventricular septum, rather than the RV free wall.

The physiologic goals of this study were twofold: The first was to determine whether levels of phosphorus energy metabolites vary with changes in RV workload. Such findings would support the hypothesis that levels of ATP hydrolysis products (i.e., ADP and/or inorganic phosphate) increase at higher workloads to serve as positive regulators of myocardial oxidative phosphorylation. Although data from isolated mitochondria and skeletal muscle support such a regulatory mechanism (10), studies of the left ventricle have yielded results which appear to depend on the age and species of animal (11–16). In large animals such as the dog (11, 15), adult sheep (12), and pig (16) increases in left ventricular workload have not been accompanied by altered levels of phosphorus energy metabolites.

The second physiologic goal of the current study was to determine the mechanisms responsible for RV failure in acute pressure overload. Unlike the left ventricle, the RV is quite limited in its capacity to respond to an acute increase in afterload. The normal human RV is unable to generate systolic pressures in excess of 50–60 mm Hg, at which point RV failure ensues. The mechanism of RV failure in acute pressure overload is uncertain, but may result from primary mechanical failure of individual contractile elements subjected to excessive load, or from ischemia of the RV wall (17, 18). Alternatively, primary energetic failure could occur, even in the absence of ischemia, if levels of RV high-energy phosphates fall or ATP hydrolysis products rise excessively at high workloads. By analogy, a major mechanism of fatigue in skeletal muscle is thought to be rising levels of inorganic phosphate (19). This study

Address reprint requests to Dr. Schwartz, Cardiology Section (111C), VA Medical Center, 4150 Clement Street, San Francisco, CA 94121.

Received for publication 6 June 1991 and in revised form 30 August 1991.

1. *Abbreviations used in this paper:* 2,3-DPG, 2,3-diphosphoglycerate; MVO_2, myocardial oxygen consumption; NMR, nuclear magnetic resonance; PCr, phosphocreatine, RV, right ventricle.

The Journal of Clinical Investigation, Inc.
Volume 89, March 1992, 909–918

sought to determine which of these mechanisms predominates in acute RV pressure overload, by simultaneous measurement of RV phosphorus metabolites, contractile function, and blood flow. In addition, blood flow measurements during adenosine infusion provided an assessment of RV coronary vasodilator reserve and the effect of increased RV perfusion on energy metabolism.

Methods

Design and testing of the right ventricular surface coil. An elliptical (3.5 × 1 cm) 2-turn phosphorus spectroscopy surface coil was specially constructed for use on the RV. The two concentric loops of the coil were cut from copper sheet (0.1 mm thickness), and configured in a crossover design. Current flows through half of the upper ellipse, crosses down to the lower ellipse (spaced 3 mm apart) to travel in the same direction completely around its circumference, and finally crosses up to complete the second half of the upper ellipse. The sensitivity profile of the coil was tested with a 2 mm diameter cylindrical glass vial filled with hydroxymethyl phosphorous triamide to a depth of 1 mm. The vial was moved in 3 dimensions with respect to the coil. At each position, the spectral intensity of hydroxymethyl phosphorous triamide was determined. The resulting spatial sensitivity profile is shown in Fig. 1. The coil lies in the y-z plane, and the x-coordinate indicates the distance from the plane of the coil. The B_0 field is directed parallel to the short axis of the coil, along the z-axis. If the coil were placed on the epicardial surface of the RV free wall, the myocardium would extend from $x = 0$ to $x = 3$–4 mm, with cavity blood present at higher values of x. As shown in Fig. 1, the coil has maximal sensitivity at $x = 0$ mm, ~ 60% of maximal sensitivity at $x = 3$ mm, and ~ 20–25% of maximal sensitivity at $x = 5$ mm. At any value of x, sensitivity declines to negligible levels within 1 cm of the boundaries of the coil in the y-z plane. These characteristics indicate that the coil would have high sensitivity in the RV free wall directly beneath it, but low sensitivity in the RV cavity or in laterally adjacent regions of myocardium (i.e., septum).

Surgical preparation and instrumentation. 20 adolescent female Yorkshire-Landrace pigs, weighing 35–41 kg, were studied. After premedication with ketamine HCl (20 mg/kg, i.m.), anesthesia was induced with α-chloralose (100 mg/kg, i.v.). After endotracheal intubation, the pigs were ventilated with 100% oxygen using a pressure cycled respirator, adjusted to maintain arterial blood pH between 7.35 and 7.45. Anesthesia was maintained with α-chloralose (20–30 mg/kg-h, i.v.). In six pigs, halothane (0.125–0.25% by inhalation) provided supplemental maintenance anesthesia. Normal saline (500 ml, i.v.) was infused rapidly with induction of anesthesia, followed by continuous infusion of 150 ml/h.

Fluid-filled introducer sheaths were inserted in both carotid arteries and advanced to the aortic arch for measurement of arterial pressure and blood gases. Via one of the sheaths, a 7-French pigtail catheter was advanced retrograde into the left ventricle for pressure measurement. A 5-French balloon-tip dual lumen catheter was advanced through a jugular vein until its tip was in a branch of the pulmonary artery and its proximal port in the RV.

The instrumentation of the heart is illustrated in Fig. 2. A median sternotomy and right lateral thoracotomy in the fourth interspace were performed, and the pericardium was opened. Fluid-filled catheters were inserted in the left and right atria through their appendages, and bipolar pacing wires were affixed to the left atrial appendage. A 20-mm diam hydraulic vascular occluder (In Vivo Metric, Healdsburg, CA) was placed around the proximal portion of the main pulmonary artery. In four pigs, a second hydraulic occluder was placed around the proximal ascending aorta. In 14 pigs, a pair of ultrasonic dimension gauges (Triton Technology, San Diego, CA) was implanted in the RV free wall, somewhat closer to the apex than to the base. The gauges were placed ~ 1 cm apart along the principal axis of shortening, as defined by Maier et al. (20). The ^{31}P surface coil was positioned slightly closer to the base than the apex of the RV, and secured to the epicardium with two loosely tied silk sutures. The positions of the dimension gauges and coil are illustrated in Fig. 2.

Segment shortening was measured with a Triton sonomicrometer. Aortic, left ventricular, right atrial and RV pressures, and RV segment

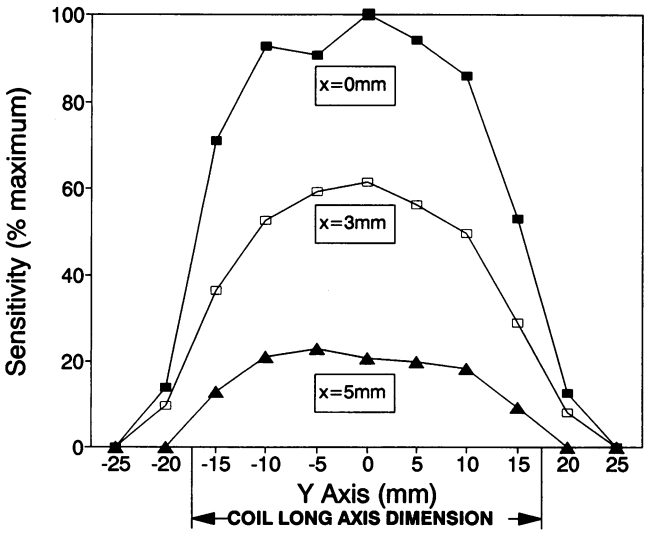

Figure 1. Sensitivity profile of the RV surface coil determined with a phantom. The coil lies in the y-z plane, with its short axis parallel to B_0 field and the z-axis. The x-coordinate corresponds to depth into the myocardium ($x < 3$–4 mm) or RV cavity ($x > 3$–4 mm). The long axis dimension of the coil (3.5 cm) is indicated on the abscissa. Note that the coil sensitivity drops sharply beyond its boundaries in the y coordinate, and at values of x exceeding the thickness of the RV free wall.

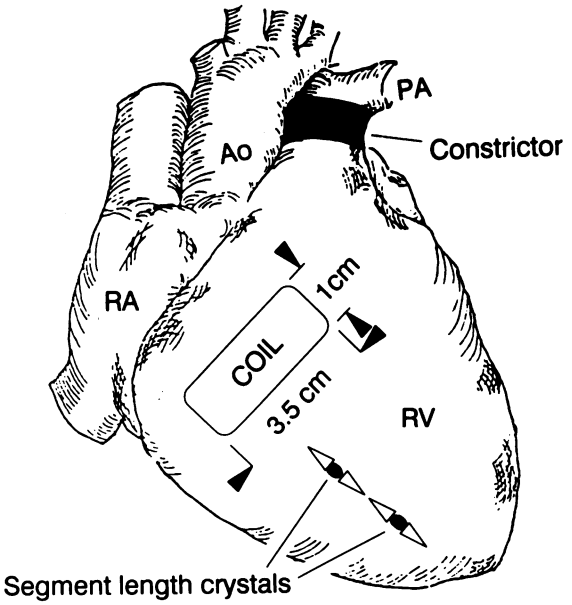

Figure 2. Instrumentation of the heart, indicating the placement of the RV surface coil and the ultrasonic dimension gauges. In addition, fluid-filled catheters were placed in the aortic arch, left ventricle, left atrium, RV, and right atrium, and pacing wires were affixed to the left atrial appendage. (Adapted from reference 20 with permission of the authors and publisher).

length were recorded on a multichannel recorder (Gould, Inc., Cupertino, CA).

Experimental protocol. During the surgical preparation, 1–2 ml of the dextran vehicle used to suspend radioactive microspheres was injected intravenously. The dextran produced a transient elevation of RV systolic pressure to 40–50 mm Hg, which persisted for 5–10 min before returning to control levels. In all cases, such pretreatment with dextran vehicle prevented any hemodynamic reactions to subsequent injections of vehicle with microspheres. At least 1 h elapsed between the test injection of dextran and the initial control measurements.

The pig was placed in a 1-m bore NMR spectrometer (Philips Medical Systems, Shelton, CT) operating at 2.0 T. To maintain body temperature, the pig was wrapped in towels and placed on a pad heated by recirculating water. The lower body was enclosed in a heavy plastic bag. In a previous series of experiments, it was determined that these measures maintained core body temperature at an average of 34°C (range 32–37°C) during prolonged, open-chest experiments. Heparin (3,000 IU, i.v.) was administered hourly to maintain catheter patency.

Control measurements of blood pressures and segment shortening were made at paced heart rates of 100, 120, 135, and 150 beats/min. Measurements were obtained at these rates so that in the event of a subsequent increase in the intrinsic heart rate, segment shortening could be compared at the same heart rate throughout the experiment. During control measurements of myocardial blood flow and ^{31}P spectroscopy, the hearts were paced at either 100 or 120 beats/min.

A control measurement of myocardial blood flow was made by injecting ~ 3 million well-mixed 15-μm-diam spheres labeled with ^{51}Cr, ^{57}Co, ^{65}Zn, ^{85}Sr, ^{95}Nb, ^{113}Sn, ^{114m}In, or ^{153}Gd (3M, Inc., St. Paul, MN) into the left atrium over 30 s. A reference arterial blood sample was simultaneously withdrawn from the carotid artery with a calibrated pump.

The magnet was shimmed on cardiac water protons to an average linewidth of 44 Hz. The radiofrequency pulse length for phosphorus spectroscopy was chosen to maximize the spectral intensity of phosphocreatine (PCr). A control ^{31}P NMR spectrum was obtained without electrocardiographic gating, using 800 acquisitions and a repetition time of 1.8 s (total acquisition time 24 min).

To assess RV coronary blood flow reserve, another injection of radioactive microspheres was performed during intravenous infusion of adenosine in 10 pigs. The infusion rate was adjusted to administer the maximal dose that did not decrease systemic arterial pressure (0.16±0.01 mg/kg-min). After the microsphere injection, the infusion was stopped and 15 min were allowed to elapse before proceeding with the experimental protocol.

Next, the hydraulic pulmonary artery constrictor was inflated gradually to produce moderate RV pressure overload (a 50% increase in RV systolic pressure, to 45±1 mm Hg). Under these conditions, measurements of hemodynamics and segment shortening were repeated with atrial pacing at the same heart rates employed during control measurements. Radioactive microspheres were injected and a ^{31}P spectrum was obtained in an identical manner to the control measurements. In the subgroup of 10 pigs, the adenosine infusion was restarted at the same dose and another injection of microspheres was made to assess RV coronary reserve during moderate pressure overload. In six pigs, a ^{31}P spectrum was also obtained under these conditions to determine if the adenosine-induced increase in RV blood flow affected levels of phosphorus metabolites during moderate RV pressure overload. 15 min were allowed to elapse after stopping the adenosine infusion before proceeding to a higher level of pressure overload.

The pulmonary artery was then constricted to produce the maximal attainable RV systolic pressure (60±1 mm Hg). Attempts to produce further pulmonary artery constriction resulted in overt RV failure, manifest by a fall in aortic blood pressure, large increases in right atrial and/or RV diastolic pressure, or significant arrhythmias. Thus, at the level of maximal pressure overload, the RV was poised on the brink of overt failure. However, systemic arterial pressure (and hence, coronary perfusion pressure) was maintained near control levels.

With maximal RV pressure overload, the measurements of hemodynamics, segment shortening, myocardial blood flow, and ^{31}P spectroscopy were repeated. Myocardial blood flow measurement and spectroscopy were also repeated during adenosine infusion in the same subgroup of pigs.

In order to increase coronary perfusion pressure and RV blood flow during maximal RV pressure overload, the proximal ascending aorta was constricted simultaneously with the pulmonary artery in four pigs. The hydraulic aortic constrictor was gradually inflated to produce a 60–100 mm Hg peak gradient between left ventricular and aortic systolic pressures. Under these conditions, repeat measurements of hemodynamics, myocardial blood flow, and ^{31}P spectroscopy were performed.

Finally the pulmonary (and aortic) constrictors were fully released. Two sequential ^{31}P spectra with accompanying hemodynamic measurements were performed 15–40 and 40–65 min after release.

At the conclusion of the experiment, the pig was killed with an overdose of sodium pentobarbital. The heart was excised and the thickness of the RV free wall in the region of the coil was measured. In studies utilizing microspheres, the heart was fixed in 10% formalin for 72 h, and then sectioned as follows. Three portions of the RV free wall were excised: at the location of the surface coil, in the apical region, and at the outflow tract. Each of these sections was divided into two equal transmural layers. Sections were also excised from the interventricular septum and the lateral left ventricular free wall. These sections were divided into three transmural layers. The tissue and reference blood samples underwent scintillation counting for calculation of regional transmural myocardial blood flow (21).

Data analysis. End-diastolic and end-systolic segment lengths and fractional systolic segment shortening were computed according to the method of Theroux et al. (22). NMR acquisitions were processed using an exponential multiplication of 15 Hz, convolution difference of 200 Hz, fast Fourier transformation, and manual phasing with zero and first order correction. Baseline flattening was performed by fitting a sixth order polynomial function to four operator-defined segments of the baseline: downfield of the phosphomonoester resonance, between the γ and α-ATP and the α- and β-ATP resonances, and upfield of β-ATP. The resulting polynomial function was subtracted from the original spectrum. This procedure makes no assumptions regarding baseline characteristics between the PME and γ-ATP resonances, where broad components and overlapping peaks may hinder baseline definition.

From the resulting spectra, peak height, linewidth, and position were determined for PCr, the three phosphates of ATP, and the combined inorganic phosphate (P_i)/phosphomonoester peak. Because of the large overlapping resonance of 2,3-diphosphoglycerate (DPG) from cavity blood, independent quantification of the intensity and chemical shift of the P_i resonance was not possible in these spectra. Spectra were further analyzed using NMR1 software (New Methods Research, Syracuse, NY) to fit Gaussian peaks for the P_i/phosphomonoester, phosphodiester, PCr, and ATP resonances. The integrated area of each of these fitted peaks was determined. NMR data are reported as the ratio of the PCr intensity to the average intensity of the α- and β-ATP resonances. Use of this ratio minimized any potential effect of wall thinning during RV pressure overload on the intensities of individual metabolites (see Discussion).

Data are reported as mean±SEM. A repeated measures analysis of variance was used to detect significant changes in hemodynamic or metabolic parameters between control, moderate, and maximal RV pressure overload, and recovery. If a significant change ($P \leq 0.05$) was detected by the F test, individual contrast analyses were performed between control, pressure overload states, and recovery (CSS software, StatSoft, Inc., Tulsa, OK). The resulting P values were corrected for multiple comparisons using the Bonferroni method (23). Differences in myocardial blood flow with and without adenosine at a given level of RV pressure were determined by a paired Student's t test.

Table I. Hemodynamics during Graded Right Ventricular Pressure Overload and Recovery

Condition	RVP		RAP	Aortic pressure			HR	EDL	ESL	Fractional segment short
	Systolic	Diastolic		Syst	Dias	Mean				
	mm Hg						*min⁻¹*	*mm*		
Control	31±1	5±1	3±1	105±5	71±3	85±3	111±3	11.8±0.5	9.2±0.5	0.21±0.02
Moderate RV pressure overload	45±1*	6±1	4±1	106±5	71±3	85±4	114±3	11.9±0.6	9.2±0.5	0.23±0.02
Maximal RV pressure overload	60±1*	9±1*	7±1*	106±5	65±3*	79±3*	128±7*	12.4±0.5*	10.0±0.5*	0.19±0.01
Recovery 15–40 min	31±1	6±1	3±1	102±4	58±4*	73±4*	151±11*	13.1±0.3*	10.9±0.3*	0.17±0.02
Recovery 40–65 min	30±1	6±1	4±1	106±4	62±5*	76±5*	139±9*	12.7±0.4*	10.2±0.4*	0.20±0.02

All data are mean±SEM. Abbreviations: RVP, right ventricular pressure; RAP, mean right atrial pressure; HR, heart rate; EDL, end diastolic segment length; ESL, end systolic segment length. Whereas spontaneous heart rate varied as shown, segment lengths were determined at a constant, paced heart rate in each pig. * Significant difference from control ($P < 0.05$), determined by analysis of variance for repeated measures followed by individual contrast analyses corrected for multiple comparisons.

Results

Hemodynamic data are shown in Table I and Figs. 3 and 4. Under control conditions, RV pressure (systolic/end diastolic) was 31±1/5±1 mm Hg, mean right atrial pressure was 3±1 mm Hg, and mean systemic arterial pressure was 85±3 mm Hg at a heart rate of 111±3 beats/min. With moderate pressure overload, RV pressure was 45±1/6±1 mm Hg, with no significant change in aortic pressure or heart rate. With maximal pressure overload, RV pressure increased to 60±1/9±1 mm Hg and mean right atrial pressure to 7±1 mm Hg. These increases in right ventricular end diastolic and right atrial pressures were statistically significant ($P < 0.001$). Systolic aortic pressure remained unchanged at 106±5 mm Hg, whereas diastolic and mean aortic pressures each declined by an average of 6 mm Hg (to 65±3 and 79±3 mm Hg, respectively, $P = 0.01$ vs. control). Heart rate increased to 128±7 beats/min ($P = 0.01$ vs. control). With release of the pulmonary artery constriction, RV pressures recovered promptly, but heart rate remained elevated with mildly reduced aortic pressure (Table I).

Sonomicrometry data are illustrated in Fig. 5 and Table I. Under control conditions, fractional RV segment shortening ([end diastolic − end systolic length]/end diastolic length) was 0.21±0.02. Despite a 50% increase in RV systolic pressure to 45±1 mm Hg with moderate pressure overload, end-systolic segment length remained constant at the average control value of 9.2 mm, with an increase in fractional segment shortening to 0.23±0.02. A constant end-systolic segment length in the face of increased afterload indicates an upward shift in the end-sys-

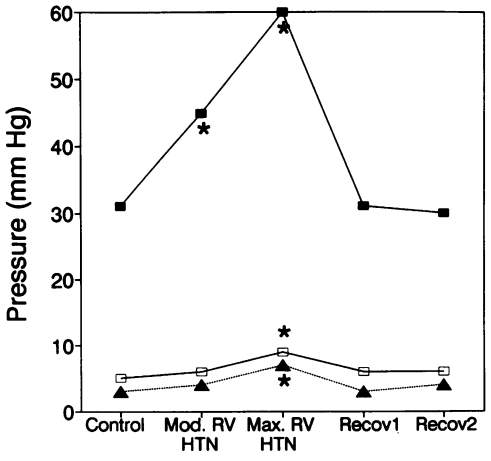

Figure 3. Right atrial and ventricular pressures during and after graded constriction of the pulmonary artery in 20 pigs. Standard errors for the data are shown in Table I. *Mod and Max RV HTN:* moderate and maximal RV pressure overload, as defined in text. *Recov1* and *Recov2*: 15–40 and 40–65 min after release of pulmonary artery constriction. *Significant change from control ($P < 0.05$, see text for statistical methods). (■) RV systolic pressure; (□) RV diastolic pressure; (▲) right atrial pressure.

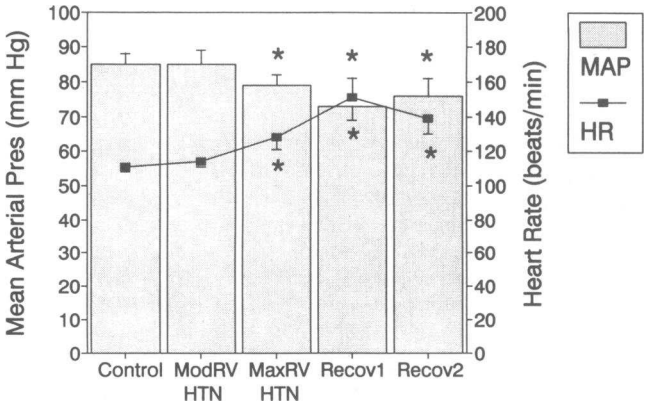

Figure 4. Systemic hemodynamics during and after graded constriction of the pulmonary artery in 20 pigs. *Mod and Max RV HTN:* moderate and maximal RV pressure overload. *Recov1* and *Recov2:* 15–40 min and 40–65 min after release of pulmonary artery constriction. *Significant change from control ($P < 0.05$). (*Shaded bars*) mean arterial pressure; (■) heart rate.

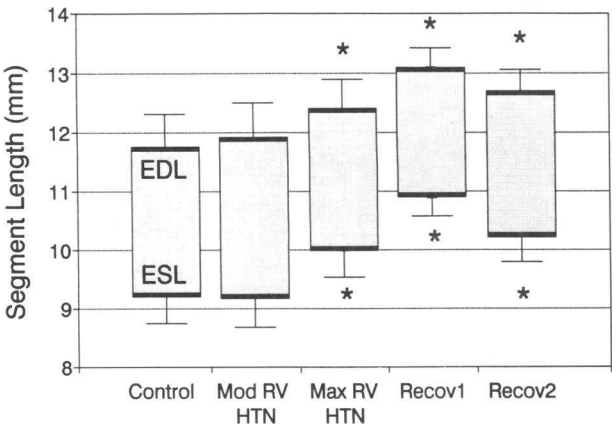

Figure 5. End-diastolic and end-systolic RV segment length measured by sonomicrometry during and after graded pulmonary artery constriction in 14 pigs. Data are mean±SEM. *Mod and Max RV HTN:* moderate and maximal RV pressure overload. *Recov1* and *Recov2:* 15–40 and 40–65 min after release of pulmonary artery constriction. *Significant change from control ($P < 0.05$). Note that contractile function is preserved despite moderate RV pressure overload.

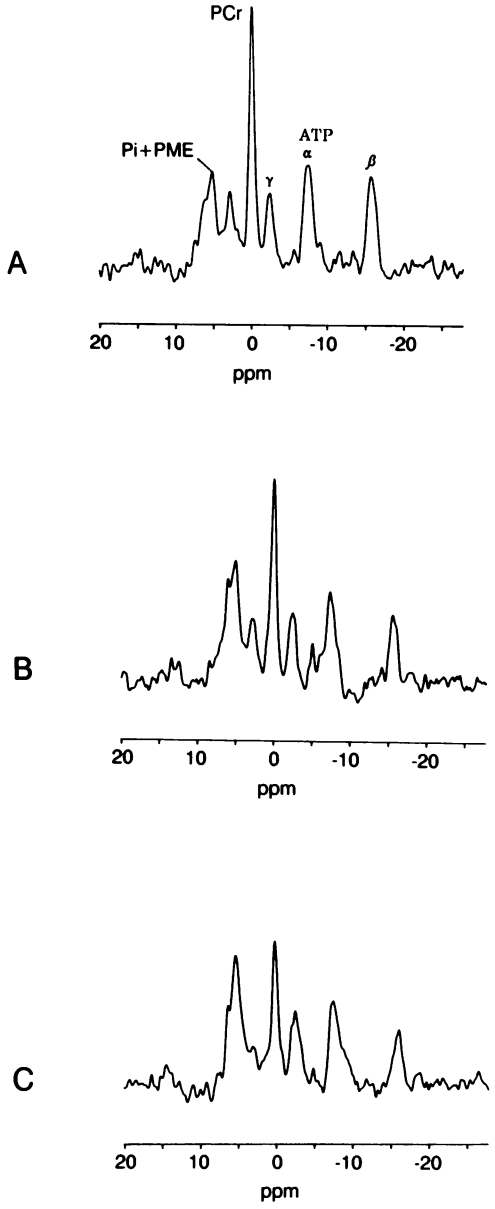

Figure 6. Representative ^{31}P spectra obtained during (*A*) Control conditions (RV systolic pressure = 28 mm Hg), (*B*) moderate RV pressure overload (RV systolic pressure = 45 mm Hg), and (*C*) maximal RV pressure overload (RV systolic pressure = 63 mm Hg).

tolic pressure/segment length relationship and, therefore, an increase in RV contractility with moderate pressure overload. This response is analogous to the Anrep effect previously described in the left ventricle (24). Maximal pressure overload (60±1 mm Hg) produced significant increases in both end-diastolic and end-systolic lengths (to means of 12.4 and 10.0 mm, respectively), with a decline in fractional segment shortening to 0.19±0.01. In the initial recovery period after release of the pulmonary artery constrictor (15–40 min), there were further increases in both end-diastolic and end-systolic segment lengths. In the second recovery period (40–65 min), both diastolic and systolic segment lengths returned partially toward their control values.

Representative ^{31}P NMR spectra obtained under control conditions and with moderate and maximal RV pressure overload are shown in Fig. 6. PCr/ATP intensity ratios from the group of 20 pigs are shown in Fig. 7. Under control conditions, signal-to-noise ratios for PCr and β-ATP were 11.8±1.8 and 6.0±0.8, respectively. The PCr/ATP ratio was 1.44±0.06, uncorrected for partial saturation effects. The PCr/ATP ratio declined significantly ($P < 0.001$) with progressive right ventricular pressure overload. Even at the moderately elevated RV systolic pressure of 45±1 mm Hg, PCr/ATP was significantly reduced to 1.28±0.06 ($P = 0.01$ vs. control). At the maximal RV systolic pressure of 60±1 mm Hg, the PCr/ATP ratio declined further to 1.17±0.04 ($P = 0.004$ vs. control, $P = 0.02$ vs. moderate pressure overload). With release of the pulmonary artery constriction, the PCr/ATP ratio returned fully to control, indicating the absence of any persistent metabolic abnormality resulting from prolonged pressure overload. Therefore, graded RV pressure overload produced a graded, reversible decrement in the myocardial PCr/ATP ratio, implying a graded increment in free ADP.

Myocardial blood flow in the inner (subendocardial) and outer (subepicardial) halves of the RV free wall are shown in Fig. 8. There were no discernible differences in blood flow to the regions of the RV directly beneath versus distant from the surface coil, indicating that the coil itself did not produce ischemia. Under control conditions, flow to the RV subendocardium and subepicardium were 1.04±0.09 and 1.37±0.11 (ml/g)/min. Flows to the right, middle, and left thirds of the septum were 1.18±0.09, 1.12±0.07, and 1.18±0.09 (ml/g)/min, respectively. Flows to the subendocardial, middle, and subepicardial thirds of the left ventricular free wall were 1.35±0.13, 1.33±0.12, and 1.11±0.08 (ml/g)/min, respectively. With moderate RV pressure overload, RV free wall blood flow increased transmurally ($P = 0.009$) to 1.89±0.27 (ml/g)/min in the subendocardium and 2.10±0.30 (ml/g)/min in the subepicardium. Flow in the right third of the septum increased to 1.89±0.37 (ml/g)/min. With maximal pressure overload, RV blood flow did not increase further in the RV subendocardium [1.72±0.14

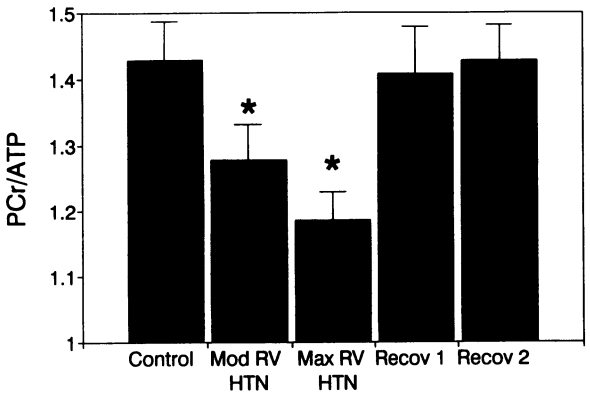

Figure 7. PCr/ATP intensity ratio calculated from ^{31}P NMR spectra during and after graded constriction of the pulmonary artery in 20 pigs. Data are mean±SEM. *Mod and Max RV HTN:* moderate and maximal RV pressure overload. *Recov1* and *Recov2:* 15–40 and 40–65 min after release of pulmonary artery constriction. *Significant change from control ($P < 0.05$). Note that progressive RV pressure overload is associated with a progressive but reversible decline in PCr/ATP.

(ml/g)/min], the RV subepicardium [1.82±0.12 (ml/g)/min], or the right third of the septum [1.89±0.24 (ml/g)/min].

Measurements of RV blood flow were made during adenosine to assess RV coronary reserve. Adenosine infusion had no

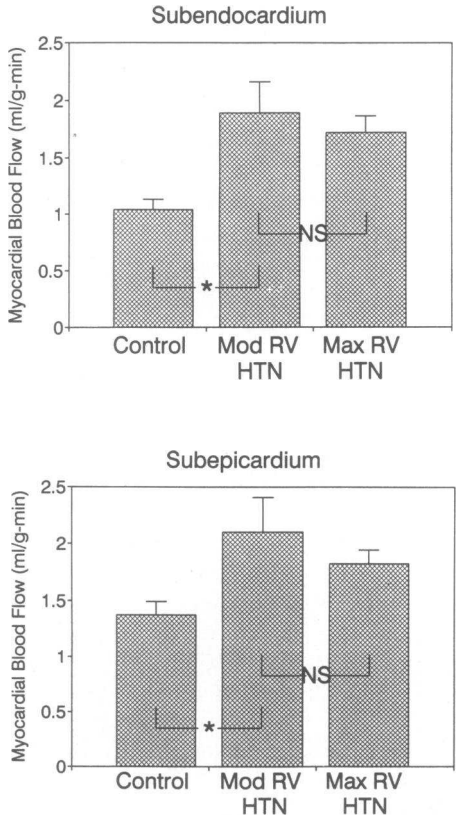

Figure 8. Myocardial blood flow to the inner (subendocardial) and outer (subepicardial) halves of the RV free wall during graded constriction of the pulmonary artery in 20 pigs. *Significant change from control ($P < 0.05$). Note that blood flow increases between control and moderate pressure overload, but does not increase further with maximal pressure overload. NS, not statistically different.

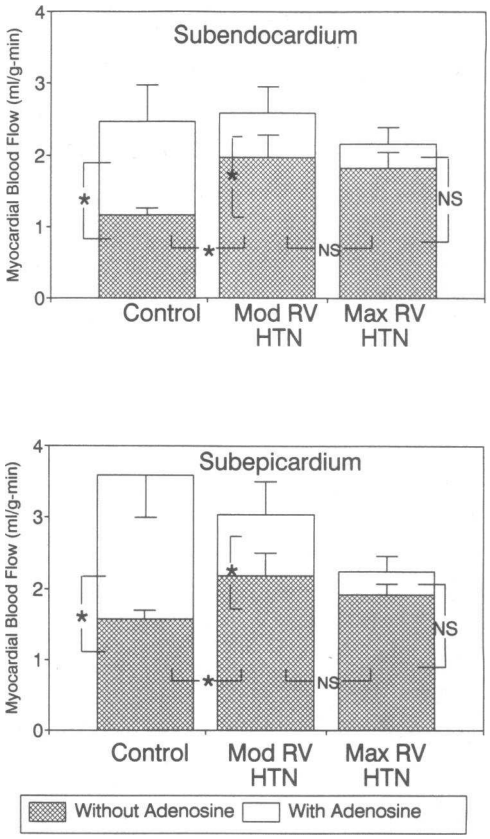

Figure 9. Incremental RV blood flow produced by intravenous adenosine infusion during graded constriction of the pulmonary artery in 10 pigs. *Significant change from control ($P < 0.05$). Note that adenosine produced significant increments in RV blood flow during moderate, but not maximal pressure overload. NS, not statistically different.

significant effect on systemic arterial pressure, heart rate, or segment shortening at any level of RV pressure. Under control conditions, adenosine increased RV subendocardial and subepicardial flows to 2.47±0.52 and 3.58±0.61 (ml/g)/min, respectively (Fig. 9). Left ventricular blood flow increased to an average of 2.32, 2.63, and 2.66 (ml/g)/min in the subendocardial, middle, and subepicardial layers. As noted before, the average adenosine dose of 0.16 (mg/kg)/min was the maximum which could be administered without a fall in systemic (coronary perfusion) pressure. This dose most likely produced submaximal coronary vasodilation, since this laboratory has obtained a 350% increase in left anterior descending coronary artery blood flow with intracoronary adenosine in a similar anesthetized pig model (25), and other investigators have found that intravenous doses closer to 1 mg/kg-min are required to produce maximal coronary vasodilation (26).

During moderate RV pressure overload, adenosine significantly incremented RV blood flow in both transmural layers, indicating persistence of pharmacologically recruitable vasodilator reserve (Fig. 9). RV subendocardial flow rose to 2.59±0.39 (ml/g)/min and subepicardial blood flow rose to 3.04±0.46 (ml/g)/min. However, when spectroscopy was repeated in a subset of six pigs during moderate pressure overload with adenosine, there was no improvement in the PCr/ATP

Table II. Effect of Aortic Constriction on Right Ventricular Blood Flow, Hemodynamics, and Energy Metabolism during Maximal Right Ventricular Pressure Overload

	RVSP	HR	Subendo MBF	Subepi MBF	PCr/ATP (control = 1.41±0.06)
	mm Hg	*min⁻¹*	*(ml/g)/min*		
Without aortic constriction	69±4	97±7	1.43±0.21	1.44±0.17	1.25±0.09
With aortic constriction	67±4	110±11	1.87±0.38	2.09±0.31	1.16±0.06

All data are mean±SEM (n = 4 pigs). Abbreviations: RVSP, right ventricular systolic pressure; Subendo, Subepi MBF, right ventricular myocardial blood flows; PCr/ATP, phosphocreatine/ATP spectral intensity ratio. Note that aortic constriction caused no improvement in PCr/ATP during maximal RV pressure overload despite an increase in perfusion.

ratio (mean value of 1.18 with and without adenosine). With maximal pressure overload, adenosine produced no significant changes in RV blood flow to either the subendocardium [2.16±0.29 (ml/g)/min] or the subepicardium [2.24±0.23 (ml/g)/min, Fig. 9]. Thus, with moderate RV pressure overload, PCr/ATP was reduced despite significant residual coronary vasodilator reserve, and PCr/ATP did not improve when RV perfusion was augmented with adenosine. However, at maximal RV pressure, RV coronary reserve was exhausted with no further increase in RV blood flow, even during adenosine infusion.

Data from the four pigs subjected to aortic constriction during maximal RV pressure overload are shown in Table II. With aortic constriction, RV subendocardial and subepicardial blood flows increased by an average of 31% and 45%. RV systolic pressure declined slightly while heart rate increased. These four pigs demonstrated no improvement in the mean PCr/ATP ratio (1.16 with aortic constriction vs. 1.25 without). Thus a modest increase in RV blood flow failed to increase the PCr/ATP ratio during maximal RV pressure overload.

Discussion

This study demonstrates for the first time that with an appropriate surface coil, in vivo ^{31}P NMR spectroscopy can provide repetitive, nondestructive measurements of high energy phosphates in the free wall of the RV.

Relationship between workload and high-energy phosphates in the right ventricle

Using this technique, the current study demonstrates that the PCr/ATP ratio varies reciprocally with afterload during graded constriction of the pulmonary artery. There are two potential explanations for this finding. A fall in PCr/ATP (implying a rise in ADP) with increasing RV workload could be a normal physiologic response through which increased concentrations of ATP hydrolysis products exert positive feedback on the rate of mitochondrial oxidative phosphorylation. Alternatively, the finding could indicate progressive ischemia of the RV free wall with pressure overload. Several pieces of evidence support the former interpretation. If ischemia caused the depression of PCr/ATP, then increased RV blood flow should have raised the ratio toward control. However, during moderate RV pressure overload, a 40% increase in RV blood flow with adenosine failed to improve the PCr/ATP ratio. It is possible that some of the decrease in PCr/ATP at maximal pressure overload was due to ischemia. However, when RV blood flow was increased by an average of 40% with aortic constriction during maximal RV pressure overload, PCr/ATP also did not increase. This finding suggests that ischemia was not solely responsible for the decline in the PCr/ATP ratio from its control level, even at maximal RV pressure overload.

The sonomicrometry data at moderate pressure overload provide further evidence against ischemia as the cause of decreased PCr/ATP. End-systolic segment length was unchanged from control, despite the increase in RV systolic pressure. A constant end-systolic segment length in the face of increased systolic pressure indicates an increase in RV contractility which would not be expected in the presence of significant ischemia.

In 1956, Chance and Williams proposed the theory of "respiratory control" of oxidative phosphorylation in studies of isolated mitochondria (27). According to this theory, an augmentation of cardiac work increases the rate of ATP hydrolysis, and raises the concentrations of ATP hydrolysis products (ADP and inorganic phosphate). ADP and inorganic phosphate then exert positive feedback on the rate of oxidative phosphorylation until the rates of ATP utilization and synthesis are matched at a higher steady-state level. Through the creatine kinase equilibrium, the PCr/ATP ratio is inversely related to the free ADP concentration (11). In addition, inorganic phosphate varies reciprocally with PCr/ATP when the latter changes with increased workload (12). Thus, the current finding of a reciprocal relationship between RV workload and PCr/ATP indicates a direct relationship between workload and ATP hydrolysis products, consistent with the theory of "respiratory control." Respiratory control of myocardial oxidative phosphorylation has been suggested by previous studies in the left ventricle of rats (13), cats (14), and neonatal lambs (12), but not in the left ventricle of large animals such as dogs (11, 15), mature sheep (12), or pigs (16). The hypothesis has not been tested heretofore in the RV.

There are several potential explanations for a difference in the metabolic responses of the right and left ventricles to increased workload. One is that intrinsic biochemical differences limit the efficiency of the RV in the generation, transfer, and/or utilization of chemical energy at high workloads. Previously reported differences in ventricular metabolism include a lower mitochondrial density in the porcine RV (3), lower capacity to oxidize substrates in rat RV (4), lower activities of lactate dehydrogenase in human RV (5), lower creatine kinase activity in the rat RV (6), and a higher α/β myosin heavy chain isoform

ratio in the RV of humans (7) and rats (8). Since the α isoform has a greater ATPase activity and a lower energetic efficiency than the β isoform, the RV might be expected to utilize ATP less efficiently than the left ventricle as workload is increased.

A limitation in the generation of chemical energy could have occurred in these experiments if the maximal achievable rate of RV oxygen consumption in vivo ($MVO_{2\text{-}max}$) was reached at an RV workload even less than moderate pressure overload. If so, further increases in RV workload would be met by an increase in glycolytic ATP production and/or phosphocreatine hydrolysis, with a consequent fall in PCr/ATP at both moderate and maximal levels of RV pressure overload. Kusachi et al. (28), studying open-chest dogs, found that regional RV oxygen consumption increased from a control value of 4 ml/100 g-min (mean RV systolic pressure 27 mm Hg) to 5 ml/100 g-min with mild pulmonary artery constriction (mean RV systolic pressure 35 mm Hg). With isoproterenol infusion, RV MVO_2 could be increased much further to 11 ml/100 g-min. While the species and experimental conditions of the two studies are not exactly comparable, the results of Kusachi et al. indicate the unlikelihood that $MVO_{2\text{-}max}$ for the RV was reached with pulmonary artery constriction less severe than the moderate level of the current study.

Mechanism of right ventricular failure in acute pressure overload

There have been several previous studies of acute RV pressure overload in intact animals. In open-chest dogs, Vlahakes et al. (17) examined RV transmural blood flow and levels of PCr and ATP in RV biopsy specimens obtained under control conditions, with RV hypertension (a doubling of RV systolic pressure to a mean of 55 mm Hg with a minimal decrease in aortic pressure), and with severe pulmonary artery constriction producing overt RV failure and marked systemic hypotension. The RV and systemic pressures at the intermediate stage of Vlahakes et al. (17) correspond to those at maximal pressure overload in the current study. At this level of pulmonary constriction, Vlahakes et al. found a 50% increase in transmural RV blood flow, similar to the current data. However, unlike the current data there remained significant coronary reserve, manifest by reactive hyperemia, and levels of high energy phosphates were unchanged from control. With the most severe pulmonary artery constriction, RV blood flow, PCr, and ATP demonstrated significant decreases, which were then reversed by normalizing systemic arterial pressure with phenylephrine. The disparity between the current results and those of Vlahakes et al. (17) may be due to a species difference in the sensitivity of RV high energy phosphates to changes in workload. Alternatively, the differences may be due to greater RV coronary reserve in the dog, in that right coronary reactive hyperemia was preserved in the dog at an RV systolic pressure of 55 mm Hg, whereas the current results with adenosine suggest depletion of RV coronary reserve in the pig at similar RV systolic pressures. Finally, a decline in RV high-energy phosphates in the absence of systemic hypotension in the current study may have resulted from a longer period of pressure overload ($\geq$1 h) than in the work of Vlahakes et al. (17).

Gold and Bache (18) measured transmural RV blood flow in conscious dogs during graded pulmonary artery constriction. As in the study of Vlahakes et al. (17), there was no evidence of RV ischemia or failure as long as systemic arterial pressure was maintained. With severe pulmonary artery constriction and systemic hypotension, RV subendocardial ischemia accompanied RV failure. However, pharmacologically recruitable coronary vasodilator reserve persisted. In a subsequent study (29), these investigators concluded that reflex adrenergic vasoconstriction was responsible for much of the RV ischemia in acute pressure overload, and could be partially reversed by α-adrenergic blockers or coronary vasodilators.

Thus, these canine studies indicated that RV ischemia could contribute to RV failure in acute pressure overload, but only when RV afterload was increased to the point of falling cardiac output, profound systemic hypotension, and reduced coronary perfusion pressure, possibly coupled with reflex coronary vasoconstriction. As long as coronary perfusion pressure was maintained at or near normal, there was no evidence of ischemia, nor of altered energy metabolism. Neither of these studies utilized a direct assessment of RV contractile function.

The results of the current study indicate that RV contractile function is maintained, or even augmented, during moderate pressure overload, despite a decline in the PCr/ATP ratio. Therefore, it is unlikely that a reduction in high-energy phosphates per se is the initiating factor in RV contractile dysfunction at the point of maximal pressure overload. Also supporting this conclusion is the observation that release of the pulmonary artery constriction resulted in prompt and complete recovery of PCr/ATP, while contractile function remained depressed (Figs. 5 and 7). Rather, the current data indicate that the onset of RV failure coincides with exhaustion of RV coronary vasodilator reserve. An important difference between the current results and those of Vlahakes et al. (17) and Gold and Bache (18) is that the current study demonstrates exhaustion of RV coronary reserve with minimal reduction in coronary perfusion pressure. These findings indicate that a doubling of RV systolic pressure, with the accompanying increase in wall tension, is a sufficient condition to limit RV blood flow in the open-chest pig with open pericardium. While the dose of adenosine employed in this study was submaximal, the lack of any incremental RV blood flow with the drug during maximal pressure overload argues against a mechanism of reflex coronary vasoconstriction. The present results do not preclude the possibility that the mechanism of RV failure in acute pressure overload is primarily mechanical (i.e., excessive tension borne by individual contractile elements limits their ability to shorten), and that exhaustion of coronary reserve is a simultaneous, but not causative event.

Limitations

Estimation of RV inorganic phosphate and pH. Because of the thinness of the RV free wall, even a coil whose sensitivity drops steeply with depth includes some chamber blood within its sensitive volume. The resulting large, broad resonance of 2,3-DPG precludes estimation of changes in RV P_i or pH in this study. However, changes in P_i are generally reciprocal to those of PCr and PCr/ATP in other interventions which perturb phosphorus metabolites.

Potential effects of RV wall thinning. The RV was visibly dilated during maximal RV pressure overload. Although a direct measurement of RV wall thickness could not be obtained in this study, it is reasonable to assume that such dilatation was accompanied by thinning of the RV free wall, with consequent reduction in the relative amount of myocardium versus

chamber blood contained within the sensitive volume of the coil. This would result in a decrease in PCr and ATP intensities and a rise in intensity in the Pi + PME region due to increased signal from 2,3-DPG in red blood cells. The use of the PCr/ATP ratio largely corrects for apparent changes in the intensity of the individual metabolites. However, because blood contains some ATP but no PCr, an increased signal from blood at the expense of myocardium would reduce ATP intensity less than PCr. Thus, the apparent myocardial PCr/ATP ratio could be spuriously reduced. The potential magnitude of this effect was estimated as follows. In spectra of fresh heparinized pig blood in vitro, the average ratio of ATP to Pi + PME intensity was found to be 0.12. In RV spectra, intensity in the Pi + PME region increased by an average of 11% and 19% during moderate and maximal RV pressure overload, compared to control. If it is assumed that all of the increase in Pi + PME was due to 2,3-DPG in blood and none to Pi in myocardium, then the additional blood ATP signal due to wall thinning would amount to ~ 2–3% of the total ATP signal. Thus, even in this worst-case calculation, increased blood ATP signal cannot account for the 11% and 19% declines in PCr/ATP observed during moderate and maximal RV pressure overload.

Potential heterogeneity of RV blood flow. In this study, RV blood flow was measured in relatively large myocardial tissue samples (≥1 g). The lack of metabolic improvement when RV blood flow was increased with adenosine or aortic constriction does not preclude the possibility that heterogeneity of blood flow existed on a smaller scale (30). If so, small areas of relative underperfusion could have coexisted in contiguity with areas of higher perfusion. Accordingly, the decline in PCr/ATP with pressure overload could have arisen from patchy ischemia in small underperfused regions, while the increased perfusion with adenosine or aortic constriction was preferentially directed to other, nonischemic areas. However, this explanation is less likely in view of data from canine left ventricle indicating that adenosine, while not eliminating heterogeneity of flow, increases flow to some extent in all regions (30). If this were the case in the RV as well, one would predict some increment in flow with adenosine, even in relatively underperfused regions, with a consequent increase in the PCr/ATP ratio. However, no change in PCr/ATP was observed when adenosine was given during moderate pressure overload in this study.

An open pericardium. This was required to secure the surface coil to the RV free wall and to insert the ultrasonic dimension gauges. It is likely that at a given level of RV systolic pressure overload, RV dilatation was more pronounced because of the lack of pericardial restraint. Accordingly, RV wall tension and MVO_2 were also likely higher than if the pericardium had been closed. Surprisingly, however, Vlahakes et al. (17) found no differences in right or left heart hemodynamics, cardiac output, RV myocardial blood flow, or right coronary reactive hyperemia in dogs subjected to graded pulmonary artery constriction with either an open or closed pericardium.

Implications

The finding that PCr/ATP in the RV decreased with increasing workload indicates that there may be energetic differences in the response of the two ventricles to increased work. Further investigation is needed to confirm that RV high energy phosphates vary reciprocally with workload when interventions other than acute pressure overload are employed. The present results are consistent with the hypothesis that exhaustion of RV coronary reserve is responsible for RV failure in acute pressure overload. However, unlike previous canine studies, the current data indicate that this may occur in the absence of a diminished coronary perfusion pressure and with elevation of the RV systolic pressure to only 60 mm Hg. Future studies of RV energetics will be aided by the repetitive, nondestructive biochemical information provided by in vivo NMR spectroscopy.

Acknowledgments

This study was supported in part by National Institutes of Health awards K11-HL02155 (Dr. Schwartz), HL-28547 (Dr. Massie), R01-AM33923 (Dr. Weiner), the Research Evaluation and Allocation Committee of the University of California, the American Lung Association, Stanford University Department of Anesthesia (Dr. Greyson), and the Veterans Affairs Medical Research Service.

References

1. Allen, D. G., and C. H. Orchard. 1987. Myocardial contractile function during ischemia and hypoxia. *Circ. Res.* 60:153–168.

2. Schwartz, G. G., S. Schaefer, D. Meyerhoff, J. Gober, P. Fochler, B. Massie, and M. W. Weiner. 1990. The dynamic relationship between myocardial contractility and energy metabolism during and following brief coronary occlusion in the pig. *Circ. Res.* 67:490–500.

3. Singh, S., F. C. White, and C. M. Bloor. 1981. Myocardial morphometric characteristics in swine. *Circ. Res.* 49:434–441.

4. Kainulainen, H., and J. Komulainen. 1989. Effects of training on regional substrate oxidation in the hearts of ageing rats. *Gerontology.* 35:289–296.

5. Lin, L., C. Sylven, P. Sotonyi, E. Somogyi, L. Kaijser, and E. Jansson. 1989. Lactate dehydrogenase and its isoenzyme activities in different parts of the normal human heart. *Cardiovasc. Res.* 23:601–606.

6. Smith, S. H., M. F. Kramer, I. Reis, S. P. Bishop, and J. S. Ingwall. 1990. Regional changes in creatine kinase and myocyte size in hypertensive and nonhypertensive cardiac hypertrophy. *Circ. Res.* 67:1334–1344.

7. Bouvagnet, P., H. Mairhofer, J. O. C. Leger, P. Puech, and J. J. Leger. 1989. Distribution pattern of α and β myosin in normal and diseased human ventricular myocardium. *Basic Res. Cardiol.* 84:91–102.

8. Brooks, W. W., O. H. L. Bing, A. S. Blaustein, and P. D. Allen. 1987. Comparison of the contractile state of myosin isozymes of rat right and left ventricular myocardium. *J. Mol. Cell. Cardiol.* 19:433–440.

9. Kantor, H. L., R. W. Briggs, and R. S. Balaban. 1984. In vivo ^{31}P nuclear magnetic resonance measurements in canine heart using a catheter-coil. *Circ. Res.* 55:261–266.

10. Chance, B., J. S. Leigh, B. J. Clark, J. Maris, J. Kent, S. Nioka, and D. Smith. 1985. Control of oxidative metabolism and oxygen delivery in human skeletal muscle: a steady-state analysis of the work/energy cost transfer function. *Proc. Natl. Acad. Sci. USA.* 82:8384–8388.

11. Balaban, R. S., H. L. Kantor, L. A. Katz, and R. W. Briggs. 1986. Relation between work and phosphate metabolite in the in vivo paced mammalian heart. *Science (Wash. DC).* 232:1121–1123.

12. Portman, M. A., F. W. Heineman, and R. S. Balaban. 1989. Developmental changes in the relation between phosphate metabolites and oxygen consumption in the sheep heart in vivo. *J. Clin. Invest.* 83:456–464.

13. Bittl, J. A., J. A. Balschi, and J. S. Ingwall. 1987. Effects of norepinephrine infusion on myocardial high-energy phosphate content and turnover in the living rat. *J. Clin. Invest.* 79:1852–1859.

14. Ligeti, L., M. D. Osbakken, B. J. Clark, M. Schnall, L. Bolinger, H. Subramanian, J. S. Leigh, and B. Chance. 1987. Cardiac transfer function relating energy metabolism to workload in different species as studied with ^{31}P NMR. *Magn. Reson. Med.* 4:112–119.

15. Robitaille, P.-M., H. Merkle, B. Lew, G. Path, K. Hendrich, P. Lindstrom, A. H. L. From, M. Garwood, R. J. Bache, et al. 1990. Transmural high energy phosphate distribution and response to alterations in workload in the normal canine myocardium as studied with spatially localized ^{31}P NMR spectroscopy. *Magn. Reson. Med.* 16:91–116.

16. Martin, J. F., B. D. Guth, R. H. Griffey, and D. E. Hoekenga. 1989. Myocardial creatine kinase exchange rates and ^{31}P NMR relaxation rates in intact pigs. *Magn. Reson. Med.* 11:64–72.

17. Vlahakes, G. J., K. Turley, and J. I. E. Hoffman. 1981. The pathophysiology of failure in acute right ventricular hypertension: hemodynamic and biochemical correlations. *Circulation.* 63:87–95.

18. Gold, F. L., and R. J. Bache. 1982. Transmural right ventricular blood flow during acute pulmonary artery hypertension in the sedated dog. *Circ. Res.* 51:196–204.

19. Vollestad, N. K., and O. M. Sejerstad. 1988. Biochemical correlates of fatigue: a brief review. *Eur. J. Appl. Physiol.* 57:336–347.

20. Maier, G. D., A. A. Bove, W. P. Santamore, and P. R. Lynch. 1980. Contractile function in canine right ventricle. *Am. J. Physiol.* 239:H794–H804.

21. Baer, R. W., B. D. Payne, E. D. Verrier, G. J. Vlahakes, D. Molodowitch, P. N. Uhlig, and J. I. E. Hoffman. 1984. Increased number of myocardial blood flow measurements with radionuclide-labeled microspheres. *Am. J. Physiol.* 246:H418–434.

22. Theroux, P., D. Franklin, J. Ross, Jr., and W. S. Kemper. 1974. Regional myocardial function during acute coronary occlusion and its modification by pharmacologic agents in the dog. *Circ. Res.* 35:896–908.

23. Miller, R. G. 1964. Simultaneous Statistical Inference. McGraw Hill, Inc., New York, 116–126.

24. Sarnoff, S. J., and J. H. Mitchell. 1961. The regulation of the performance of the heart. *Am. J. Med.* 30:747–771.

25. Schwartz, G. G., S. Schaefer, S. D. Trocha, J. Garcia, B. Massie, and M. W. Weiner. 1990. Can myocardial energetics be augmented by supranormal coronary blood flow? Society of Magnetic Resonance in Medicine, 9th Annual Meeting, p 1242. (Abstr.)

26. Rembert, J. C., L. M. Boyd, W. P. Watkinson, and J. C. Greenfield, Jr. 1980. Effect of adenosine on transmural myocardial blood flow distribution in the conscious dog. *Am. J. Physiol.* 239:H7–H13.

27. Chance, B., and C. M. Williams. 1956. The respiratory chain and oxidative phosphorylation. *Adv. Enzymol.* 17:65–134.

28. Kusachi, S., O. Nishiyama, K. Yasuhara, D. Saito, S. Haraoka, and H. Nagashima. 1982. Right and left ventricular oxygen metabolism in open-chest dogs. *Am. J. Physiol.* 243:H761–H766.

29. Gold, F. L., L. D. Horwitz, and R. J. Bache. 1984. Adrenergic coronary vasoconstriction in acute right ventricular hypertension. *Cardiovasc. Res.* 18:447–454.

30. Austin, R. E., Jr., G. S. Aldea, D. L. Coggins, A. E. Flynn, and J. I. E. Hoffman. 1990. Profound spatial heterogeneity of coronary reserve: discordance between patterns of resting and maximal myocardial blood flow. *Circ. Res.* 67:319–331.